

Numerical Estimation of Convective Heat Transfer Coefficient and Heat Flux for a Supersonic Rocket Nozzle

Amit Makhija^{#*}, Kowsik Bodi[#] and Debasis Chakraborty[§]

[#]Indian Institute of Technology, Bombay, Mumbai - 400 076, India

[§]Mahindra University, Hyderabad - 500 043, India

*E-mail: makhijaamit0909@gmail.com

ABSTRACT

Rocket nozzles are often cooled by passing liquid propellants through channels in the nozzle walls. Estimating heat transfer to the wall from the hot gases in the nozzle is essential in deciding on the coolant flow requirements. The present work examines the computational estimation of convection heat transfer to the nozzle walls for compressible turbulent flows. Computations were performed using the *rhoPimpleFoam* solver in OpenFOAM® with two different turbulence models. We simulate the supersonic flow over a flat plate and validate the heat flux calculation method and turbulence model characteristics. We compare two methods of calculating convection heat transfer in the context of the nozzle flow case presented by Back & Massier. We find that the *realizablek-ε* turbulence model works well in estimating the heat transfer coefficient.

Keywords: Rocket nozzle; Supersonic flow; Flat plate; Convective heat transfer, OpenFOAM®

1. INTRODUCTION

Designing robust and optimized cooling systems that can permit rocket combustor and nozzle walls to withstand extremely high aero-thermal loads is a formidable challenge to the propulsion community. In reality, in high-speed engines, flow field, shock boundary layer interaction, vortex formation, and chemical reactions influence the thermal field near the wall, making the analysis formidable¹. The heat transfer in aerospace engines is also affected by transient phenomena (e.g., instabilities, SBLI, etc.), and reliable heat transfer calculation is essential for selecting the appropriate structural materials². Computational studies typically consider the limiting cases of adiabatic or isothermal walls. However, in practice, wall temperature values are determined by the finite heat transfer between the flow and the wall material. The wall temperature also changes continuously in response to the transient flow phenomena. Moreover, this transient response of the wall materials can affect the flow fields. An additional factor that affects heat transfer calculations is the temperature dependence of the thermophysical properties of the fluids³⁻⁴.

Back, *et al.*⁵ experimentally studied the convective heat transfer in a nozzle and reported measurements that have been used to evaluate computational models in the prediction of heat transfer. They performed the studies with cooled and uncooled nozzle walls at various stagnation pressures and temperatures for supersonic outlet conditions of Mach number around 2.6. They found that calculating momentum or energy thickness is sufficient to predict the heat transfer coefficient to a great degree. However, this formulation is unsuitable if the

flow is separated at some point. They also performed several numerical studies and found that there needs to be a global empirical correlation to estimate the convective heat transfer for different pressure gradients or inlet pressure conditions.

Bartz,⁶⁻⁷ provided an approximate solution to the supersonic nozzle, including curvature effects; however, the correlation was limited to some specific categories of flows. Nichols and Nelson⁸ performed the numerical investigation on the same nozzle geometry using a modified Crocco-Busemann⁹ equation. They concluded that the low-Reynolds number wall function with $y^+ < 100$ should be able to predict the heat transfer coefficient along the wall. Dharavath¹⁰, *et al.* also performed the numerical study incorporating Kader's¹¹ formulation. They succeeded in capturing the heat transfer coefficient using ANSYS® Fluent. They also reported that the placement of the first cell near the wall strongly affects heat transfer prediction. A similar study by Zhalehrajabi¹² compared the effect of a number of grids and a turbulence model. They reported that heat flux estimation is grid sensitive, and results obtained using the *k-ε* turbulence model¹³ are close to the experimental data than the *k-ω* SST¹⁴⁻¹⁵ turbulence model.

Most studies in the literature have been done using commercial or proprietary CFD tools. In the present study, initially, we study the heat transfer phenomenon over a flat plate to validate the heat flux estimating methods and turbulence models. We evaluate the capability of the open-source CFD tool OpenFOAM® in simulating heat transfer in compressible turbulent nozzle flows. We use the nozzle heat transfer data of Back⁵, *et al.* for validating the solver and comparing the different turbulence models and calculation methods for turbulent wall heat flux. One source of ambiguity

while comparing with the heat flux data reported by Back, *et al.*^{5,13,14} is the absence of an accurate description of the non-uniform wall temperature. This is another issue that we attempt to address in this work.

2. HEAT TRANSFER AND HEAT FLUX ESTIMATION METHODS

To predict the heat transfer coefficient, we considered the following two approaches:

- Modified Crocco-Busemann equation⁹ (method-1): The temperature distribution within the boundary layer is given by:

$$T(x) = T_w(1 + \beta u^+ + \Gamma(u^+)^2) \quad (1)$$

where, $T(x)$ is taken as the centreline temperature, T_w is wall temperature, β shall be called a heat transfer function, and is given by

$$\beta = \frac{\dot{q}_w \mu_w}{\rho_w T_w \lambda_w u_w} \quad (2)$$

where, \dot{q}_w is wall heat flux, μ_w is dynamic viscosity near the wall, ρ_w is fluid density near the wall, λ_w is the thermal conductivity of the fluid near the fluid and u_w is friction or shear velocity is given as $\sqrt{\tau_w/\rho_w}$ and the non-dimensional velocity (u^+) can be written as $\bar{u}\sqrt{\rho_w/\tau_w}$. Here, \bar{u} is the average fluid velocity or velocity parallel to the wall, and τ_w is wall shear stress. Γ represents the compressibility effects and is estimated as

$$\Gamma = \frac{ru_\tau^2}{2c_p T_w} \quad (3)$$

where, r is the recovery factor, given as $\text{Pr}^{1/3}$ for turbulent flows, however, in the current test case, it is considered a constant of 0.89⁵ and c_p is the specific heat at constant pressure.

With this method, wall heat flux is initially estimated, and then the heat transfer coefficient is calculated using the formula as follows.

$$h = \frac{\dot{q}_w}{T_w - T_{ad}(x)} \quad (4)$$

where, $T_{ad}(x)$ is the adiabatic wall temperature, which is given by:

$$T_{ad}(x) = T(x) \left[1 + r \left(\frac{\gamma - 1}{2} \right) M_\infty^2 \right] \quad (5)$$

here, γ is 1.345⁵, M_∞ is referred to as the Mach number along the centreline, and x is a location in the axial direction.

- Using inertial sub-layer theory (method-2): We consider the non-dimensional velocity is given by $y^+ = u^+$, with the first grid point placed in the near wall or sub-layer region ($0 < y^+ < 5$)¹⁸.

From Fourier's law of conduction, the wall heat flux is

$$\dot{q}_w = -\lambda_w \frac{\partial T}{\partial n} \quad (6)$$

This expression is approximated as:

$$\dot{q}_w = -\lambda_w \frac{(T_w - T_{ad}(x))}{\Delta n} \quad (7)$$

where, Δn is the first point distance from the wall. Further, Δn

and λ_w shall be eliminated using the below correlation of the y^+ factor and Prandtl number (Pr).

$$y^+ = \frac{\rho_w \Delta n u_\tau}{\mu_w} \quad \text{Pr} = \frac{\mu_w c_p}{\lambda_w} \quad (9)$$

$$-\frac{\dot{q}_w}{(T_w - T_{ad}(x))} \equiv h = \left(\frac{u_\tau}{y^+} \right) \frac{\rho_w c_p}{\text{Pr}} = \left(\frac{u_\tau}{u^+} \right) \frac{\rho_w c_p}{\text{Pr}} \quad (10)$$

In literature, the term in the denominator of the equation, i.e., $y^+ \text{Pr}$ is often denoted by either T^+ or θ^+ ¹¹ and different sets of equations are defined to estimate the same. However, in the present case, as per the underlying theory¹⁸, the y^+ shall be replaced with u^+ as shown in Eqn. (10). In contrast to the first method, we estimate the heat transfer coefficient and then calculate the heat flux using Eqn. (4).

3. SIMULATION DETAILS AND NUMERICAL METHODOLOGY

The gas is considered thermally perfect, having the thermophysical properties of air. The dynamic viscosity is defined by Sutherland's law¹⁹⁻²⁰

$$\mu = \frac{A_s \sqrt{T}}{1 + T_s/T} \quad (12)$$

where, $A_s = 1.67212 \times 10^{-6} \text{ m}^2/\text{s}^2$ and $T_s = 170.672 \text{ K}$ are constants.

3.1 Supersonic Flow over a Flat Plate - A Validation Study

A preliminary canonical problem has been studied to validate and choose the appropriate turbulence model and grid(s). Also, to authenticate that the methods discussed in Section 2 are promising to estimate wall heat flux/transfer. The flat plate with a length (L), height (H), and width (W) of 88 cm, 21 cm, and 2 mm was simulated using *realizablek-ε* and *k-ω* SST turbulence models with the inlet free-stream²¹⁻²² parameters of $M_\infty : 2.80$, $\text{Re}_\infty : 7.5 \times 10^7$, $P_\infty : 26085 \text{ N/m}^2$, $T_\infty : 99.82 \text{ K}$, and the wall temperature (T_w) was kept constant at 270.89 K. The grids are refined near the wall by providing a biasing factor of 1000 with a stretching factor of 1.02; hence, the average y^+ factor is less than 0.05 in any of the simulations. A zero gradient condition was applied at the outlet boundaries in view of the outflow being supersonic.

3.2 Supersonic Flow in a Nozzle

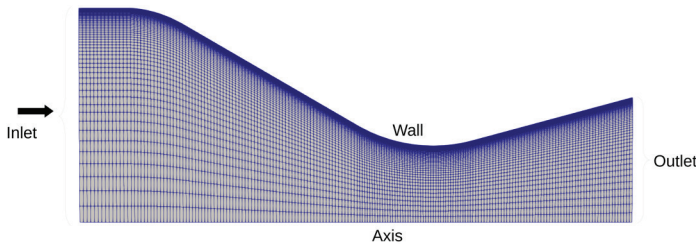
The nozzle geometry details are provided in Table 1. The domain with meshing is shown in Fig. 1. This study has compared the two turbulence models, *realizablek-ε* and *k-ω* SST turbulence models at different wall temperatures. The total number of cells in the x and y directions are 188 and 96, respectively. Here, the first cell is placed at a distance of 1 μm from the wall, and the average y^+ factor is 0.5. The placement of the first cell point at 1 micron height was also reported by Dharavath, *et al.*¹⁰ for estimating the wall heat flux rate.

3.2.1 Adiabatic Wall Case

Computations in the present work use *rhoPimpleFoam*²³, a transient solver in the OpenFOAM® v9 framework for

Table 1. C-D nozzle geometry details⁵

Parameter	Value
Length of the nozzle	0.1505 m
Inlet radius & outlet radius	0.064m & 0.0373 m
Throat radius&its location	0.0229 m & 0.091 m
Convergent & divergent half angles	30°& 15°
Expansion & contraction area ratio	2.68 & 7.75
The radius of curvature at the inlet	0.0607 m
The radius of curvature at the throat	0.0457 m


Figure 1. Axisymmetric two-dimensional C-D nozzle sector (wedge angle = 1°) with meshing.

simulating turbulent compressible fluids and flows. It uses the flexible algorithm PIMPLE²³ for the simulations, a blend of the SIMPLE (Semi-Implicit Method for Pressure Linked Equations) and PISO (Pressure-Implicit with Splitting Operators). In order to validate the *rhoPimpleFoam* solver capability, a test case was adopted where flow separation exists to ensure that the solver is capturing the flow and thermal fields with accuracy for transonic/supersonic flows. At the inlet, the total temperature (T_0) is 835 K and the total pressure (P_0) is 308885 N/m². All outlet boundaries except for pressure were exposed with zero gradient boundary conditions, whereas outlet pressure was set to wave transmissive²³, which is suitable for flow separation cases. No slip boundary condition is used for the wall.

3.2.2 Isothermal Wall Case

In contrast to the previous test case, the aim is to estimate the wall heat transfer. Therefore, a test case was chosen where the flow in the C-D nozzle is a fully expanded case. At the inlet, the total temperature (T_0) is 824.4 K and the total pressure (P_0) is 1038350.4 N/m². In this case, the flow exited at supersonic speed; hence, the pressure outlet boundary condition was also set to zero gradient. The study is conducted with three different constant wall temperatures, i.e., 486, 500, and 550.

3.3 Computational Resource Details

All the simulations were carried out in the cluster “SHUKRA” of the Aerospace Computational Engine (ACE) High-Performance Computing (HPC) facility of the Aerospace Engineering Department, IIT Bombay. We used one node of AMD Ryzen 3950x processor with 16 CPUs (1 GB memory per CPU). The steady state was achieved in the nozzle at 0.01 seconds of the simulation runtime, which took less than 20 minutes of computation time. However, to ensure that the flow had been developed and is not being affected, we simulated for 0.1 sec., which took approximately three hours.

4. RESULTS AND DISCUSSIONS

4.1 Flat Plate Boundary Layer (Zero Gradient)

In this test case, we aim to compare and study the acceptability of existing heat transfer heat transfer/flux calculation methods and the different turbulence models. Figure 2 shows the pressure variation along the wall and in the direction normal to the wall. This variation is much larger for the $k-\omega$ SST model simulation than for the *realizable* $k-\epsilon$ model.

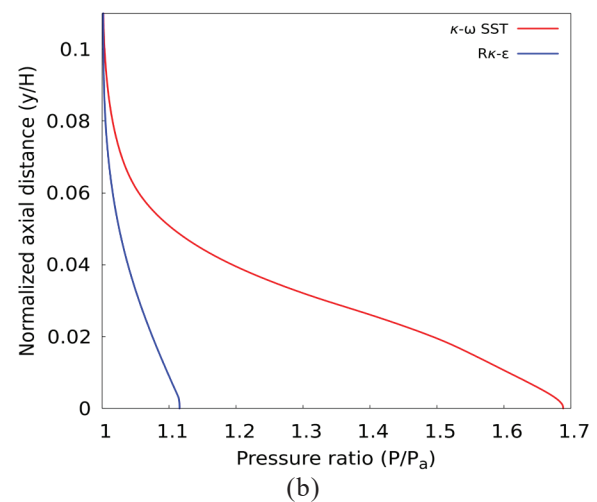
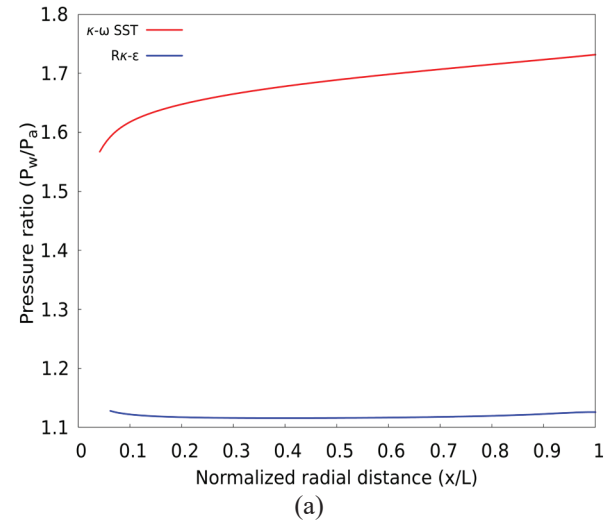

Figure 2. Normalized wall pressure comparison for different turbulence models (a) along the wall and (b) normal to the wall at the center of the domain.

Figure 3 shows the comparison and variation of wall heat flux along the flat plate with heat flux calculation method-1. We note that both models predict different wall heat flux and shear stress; hence, the numerical values differ in both cases.

We also compared the velocity profiles and the variation of skin friction coefficient along the wall (not presented here). We found that the *realizable* $k-\epsilon$ model predictions agree with the expected profiles for the turbulent boundary layer. The $k-\omega$ SST predicts a much larger boundary layer thickness than expected. Furthermore, we compare the results of the numerically obtained wall heat flux with the heat flux calculation method-1 discussed in Section 2. We found a relatively high difference in skin friction coefficient values, which is expected to affect the wall heat flux values.

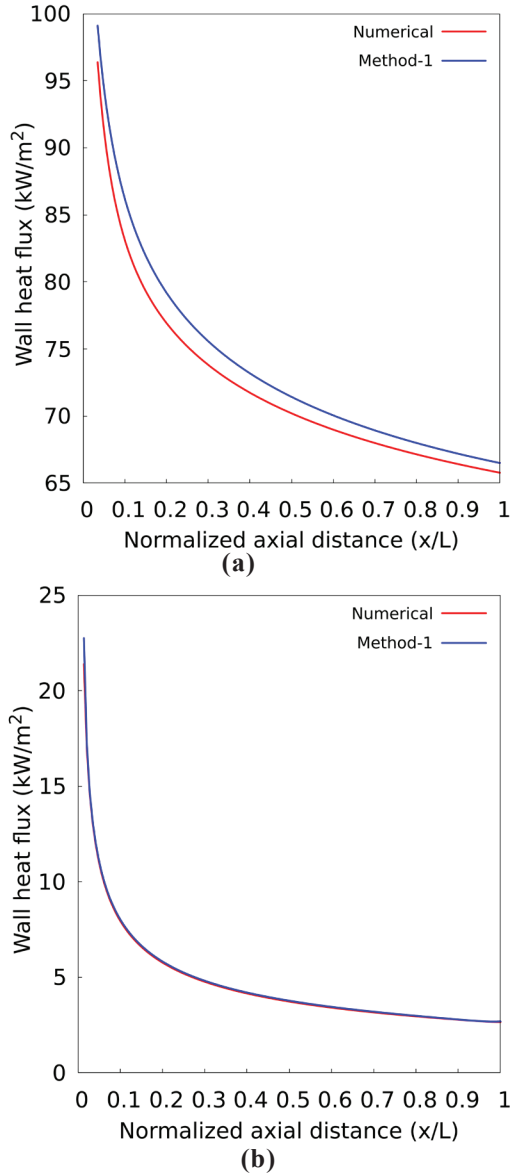


Figure 3. Heat flux variation along the wall for (a) $k-\omega$ SST and (b) $k-\epsilon$ turbulence models.

Our observation is restricted to the use of the $k-\omega$ SST turbulence model for the solver *rhoPimpleFoam*, as satisfactory performance has been observed while using the same turbulence model with the density-based solver in OpenFOAM (*rhoCentralFoam*²³) in simulating the hypersonic flow over a compression corner and diamond airfoil²⁴⁻²⁵, where the predicted wall heat flux agrees well with the experimental data.

4.2 Supersonic Flow in a Nozzle

In the present test case, we have used the *rhoPimpleFoam* solver with the *realizablek-ε* turbulence model, a two-equation model with the maximum Courant number of 0.5. This model accurately simulates turbulent boundary layers, including situations with adverse pressure gradients, separated flows, and recirculation zones.

Initially, the adiabatic wall test case was simulated to validate the solver. The grid independence study was made

to ensure accuracy. All the results presented for this test case are at a steadystate. Figure 4 shows the grid independence study and compares the normalized pressure results with the experimental data of the numerical simulation for the adiabatic wall case. The parameter on the y-axis is the ratio of static wall pressure to the stagnation pressure, and the x -axis refers to the non-dimensional axial distance. It can be observed that there is a marginal difference between the results of the latter two meshes. Therefore, mesh-2 (blue line) was chosen to present the results. The excellent match between the numerical results and experimental measurements confirms that the mesh and boundary conditions are appropriate for the study. The present study can capture the shock location on the wall, and a jump shall be observed at the normalized location of 0.8. After validating the solver using the *realizablek-ε* turbulence model, we examined the accuracy of the $k-\omega$ SST model. However, the $k-\omega$ SST model predictions do not agree well with the experimental data.

In both simulations, the average y^+ is kept below 1.2. A biasing factor of 0.001 in the y -direction has been provided to maintain thermal conductivity uniform and constant along the first grid point placed at a distance of 4 μm from the wall. The motive behind such a condition was to make the dependency of wall heat flux calculations only on the temperature and cell width function.

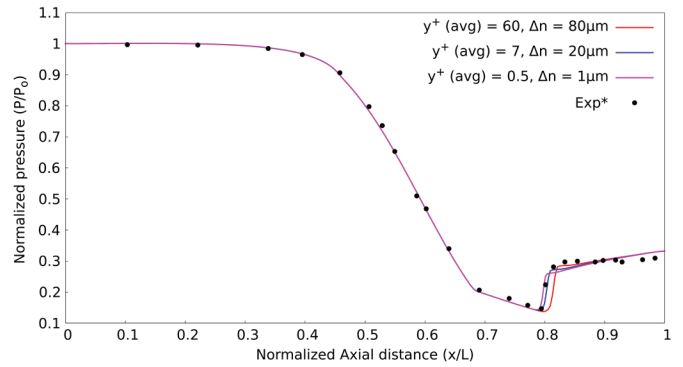


Figure 4. Grid independence study and comparison of numerically obtained static (pressure on the wall) to stagnation pressure ratio with the experimental (Exp*)¹⁶ data along the nozzle for adiabatic wall case.

Figure 5 shows the static and stagnation pressure ratio along the wall to the experimental data¹⁶.

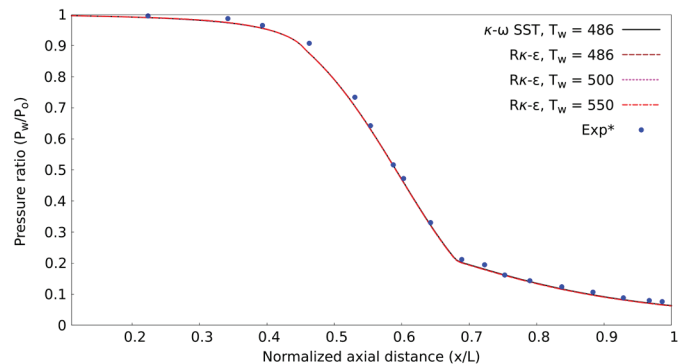


Figure 5. Comparison of predicted temperature at the radial location of 0.02 m to the experimental (Exp*)¹⁶ data along the nozzle.

Similarly, we have reported and compared the flux ($\phi = \rho u$) variation with the experimental data shown in Fig. 6. However, the match for the above two cases was found at a radial distance of 0.02 m from the nozzle axis. The agreement is good for all three variables, and the deviation can be attributed to the large grid aspect ratio in the region away from the wall. As mentioned previously, the nozzle is being cooled, which means the wall temperature will be different than the uncooled wall. However, here we are considering the wall at a constant temperature. It can be seen that there is no separation (adverse pressure gradient) in the flow, and the outflow is supersonic. The pressure profile is the same irrespective of wall temperature in the pressure plot (Fig. 5). Also, it does not affect the far field, as shown in Fig. 6.

However, the wall temperature will impact the wall heat flux as we have maintained the thermal conductivity of the fluid approximately constant near the wall, and the variation in the estimation concerning the wall temperature shall be seen in Fig. 7. We can observe that the wall temperature significantly impacts the throat and the divergent section. Irrespective of wall temperature, we are underpredicting the wall heat flux at the divergent section. The reason could be the assumption of the same wall temperature throughout the nozzle. Further, with the help of estimated wall heat flux, we calculated the heat transfer coefficient using Eqn. 4, and the results are shown in Fig. 8 and compared with the experimental data¹⁷.

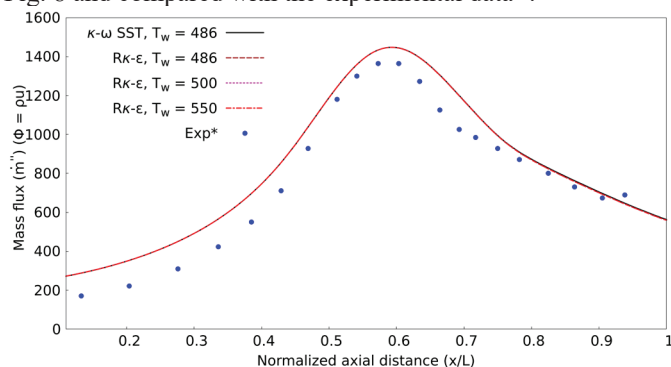


Figure 6. Comparison of predicted flux at the radial location of 0.02 m to the experimental (Exp*)¹⁷ data along the nozzle.

It can be seen that the heat transfer coefficient results agree better with the experimental data. The maximum percentage error is 45 %, whereas the average error is nearly 20 %. The disagreement in the results can be due to many factors. The conduction through the wall and further convection from the wall to the coolant are neglected. Also, radiation heat transfer is absent in the present case.

We presented the heat flux and heat transfer coefficient results using the first approach mentioned in Section 2. Hereafter, an effort is made to compare the effects of method-1 (Modified Crocco-Busemann equation) and method-2 (sub-layer theory).

The comparison is shown in Fig. 9. There is no difference in the predicted heat transfer coefficient on the convergent section; however, a minimal deviation is seen in the throat and divergent sections. This inconsistency may be due to not capturing the compressibility effects appropriately²⁶.

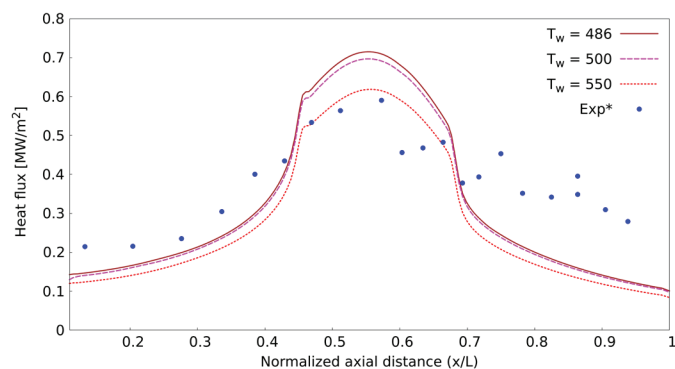


Figure 7. Comparison of predicted wall heat flux using modified Crocco-Busemann equation with the experimental (Exp*)¹⁷ data for different wall temperatures.

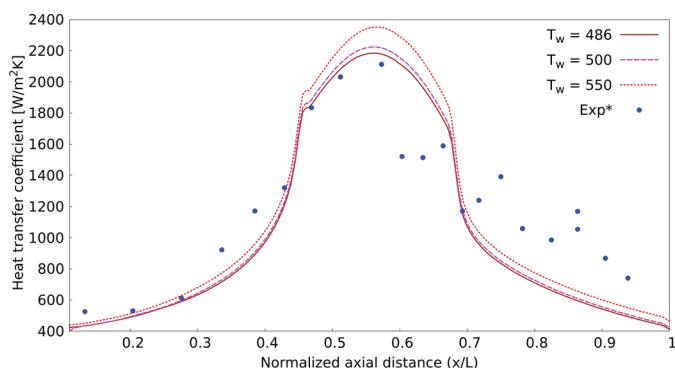


Figure 8. Comparison of predicted heat transfer coefficient using modified Crocco-Busemann equation with the experimental (Exp*)¹⁷ data for different wall temperatures.

We also carried out the simulation with the $k-\omega$ SST turbulence model for the same test case. The average y^+ factor is 1.3 and maintained constant thermal conductivity of the fluid near the wall. The heat transfer coefficient results with both methods are shown in Fig. 9(b). The values are highly overpredicted. It is evident from the results that the $k-\omega$ SST turbulence model is not suitable for estimating the heat transfer coefficient in the *rhoPimpleFoam* solver for this constant wall temperature condition in the present work. Therefore, we preferred the *realizablek-epsilon* over the $k-\omega$ SST turbulence model for other test cases.

Furthermore, the study was extended to identify the effect of grids on the wall heat transfer coefficient estimation. The number of grids doubled in the complete domain. Now, the first cell height is 0.5 μm , and the corresponding y^+ factor near the wall is 0.2. We found that the wall pressure prediction was precisely the same as reported in Fig. 5 (not presented here), irrespective of grids. However, a slight variation was reported in the prediction of the heat transfer coefficient, as presented in Fig. 10. A similar observation was made in literature¹⁰.

To ensure the acceptability of results reported for the total pressure of 10.2 bar, we continued our simulation for the total pressure of 5.12 bar with a stagnation temperature of 845 K. In this case, the shock/flow separation also does not exist in the divergent section. The predicted heat transfer coefficient results are shown in Fig. 11, where a comparison has been

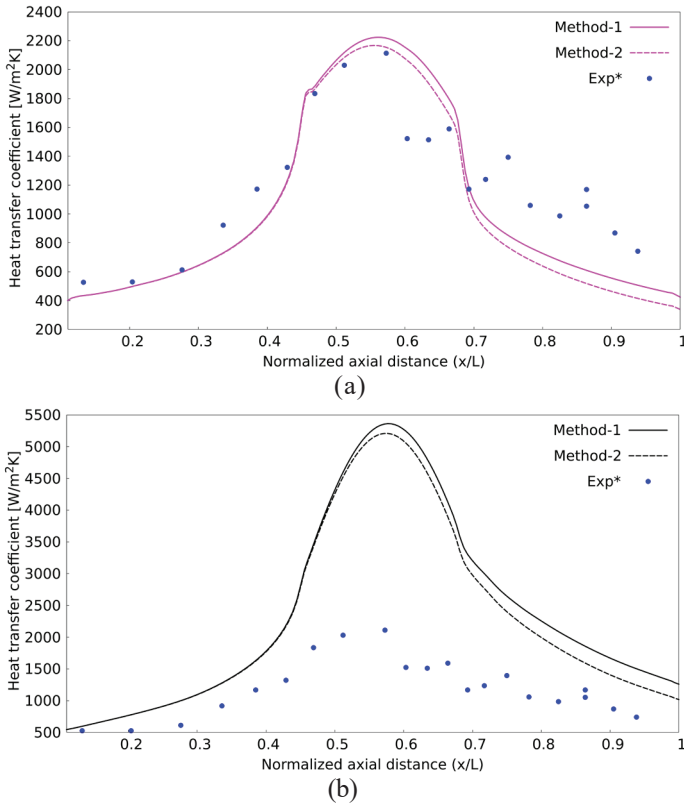


Figure 9. Comparison of predicted heat transfer coefficient estimated through method-1 and method-2, and to the experimental (Exp*)¹⁷ data with $T_w = 500$ K for (a) $k-\epsilon$ and (b) $k-\omega$ SST turbulence models.

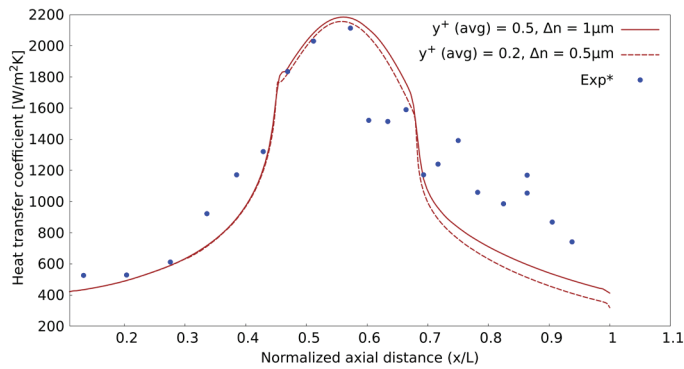


Figure 10. Comparison of predicted heat transfer coefficient for two different grids with the experimental (Exp*)¹⁴ data for $T_w = 486$ K.

made between the estimations of the two methods and the experimental data. We find a significant difference between the computed and measured values for the heat transfer coefficient for the case of the total pressure of 10.2 bar. In this case, we obtain a similar disagreement for the heat transfer coefficient in the throat and divergent section.

The possible reasons for disagreement in the heat transfer coefficient would be due to the assumption of isothermal wall conditions. The nozzle walls were water-cooled in the experiments. This effect was not considered in our computations. Wall conduction heat transfer was also not considered as wall conductivity, and coolant determines the

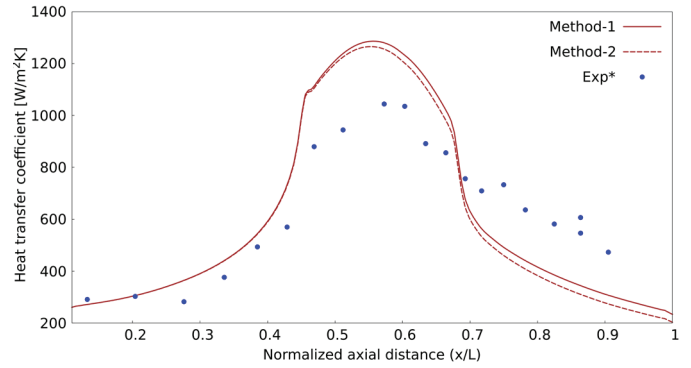


Figure 11. Comparison of predicted heat transfer coefficient estimated through method-1 and method-2 and to the experimental (Exp*)¹⁴ data for $P_0 = 5.12$ bar and $T_0 = 845$ K.

wall temperature variation, hence the heat transfer from the gas flow to the nozzle walls. Back, *et al.*⁵ provide a specific temperature range for the nozzle wall temperature; however, how the temperature varies along the nozzle wall is unknown and hence is the source of uncertainty for computational studies on this problem.

5. CONCLUSIONS

Supersonic flow over a flat plate was simulated in order to validate the heat flux estimation methods and turbulence model. A supersonic-cooled wall nozzle has been simulated with constant wall temperature conditions using the *rhoPimpleFoam* solver in the OpenFOAM® framework. The wall pressure, temperature field, and mass flux results agree well with the experimental data. In contrast, the heat flux and heat transfer agree reasonably. We have tried to simulate the nozzle with different wall temperature and turbulence models. Two methods were used to calculate the heat transfer coefficient. Method-1 uses the Modified Crocco-Busemann⁹ equation, and method-2 uses the inertial sub-layer theory. The obtained results were compared with the experimental data. The study was extended to observe the variation in the estimation of heat transfer by varying the grid size or refining the grids. Further, the behaviour of numerical results was validated with another fully expanded nozzle case for the pressure of 5.12 bar.

The study aims to estimate the convective heat transfer with different assumptions and formulations. It was found that the wall temperature of 486 K or 500 K is suitable for the primary set of results of the total inlet pressure of 10.2 bar. We also found the results of the $k-\omega$ SST turbulence model disagree with the experimental data, and the *realizable*- $k-\epsilon$ turbulence model was found most suitable for the supersonic flows. Both methods estimate nearly the same heat transfer coefficient if the average y^+ factor lies in the inertial sub-layer region where laminar flow dominates.

6. FUTURE WORK

The study may be further extended considering the fluid-structure interaction to validate if the cause is an incorrect wall boundary condition. Therefore, a conjugate heat transfer study would be more appropriate to estimate the wall heat flux and heat transfer coefficient. Further studies may also be directed

to investigate the reasons for the significant errors in k - ω SST simulations done using *rhoPimpleFoam*.

REFERENCES

- Jiang, J.; Ling Zhang, R.; Ling Le, J.; Xiong Liu, W.; Yang, Y.; Zhang, L. & Zhu Zhao, G. Regeneratively cooled scramjet heat transfer calculation and comparison with experimental data. *In Proceedings of the Institution of Mechanical Engineers, Part G: J. Aerospace Eng.*, 2014. **228**(8), 1227–1234. doi:10.1177/0954410013488737.
- Elliott, D.G.; Bartz, D.R. & Silver, S. Calculation of turbulent boundary layer growth and heat transfer in axisymmetric nozzles. Jet Propulsion Laboratory, California Institute of Technology, Technical Report No. 32-387. February 1963.
- Ramasamy, D.; Appusamy, A. & Narayanan, A. Review of the wall temperature prediction capability of available correlations for heat transfer at supercritical conditions of water. *J. Energy*, 2013. **2013**. doi: 10.1155/2013/159098.
- Wang, Z. & Turan, A. Influence of non-uniform wall heat flux on critical heat flux prediction in upward flowing round pipe two-phase flow. *Int. J. Heat and Mass Transfer*, 2021. **164**, 120619. doi:10.1016/j.ijheatmasstransfer.2020.120619.
- Back, L.; Massier, P. & Gier, H. Convective heat transfer in a convergent-divergent nozzle. *Int. J. Heat and Mass Transfer*, 1964. **7**(5), 549–568. doi: 10.1016/0017-9310(64) 90052-3.
- Bartz, D.R. An approximate solution of compressible turbulent boundary-layer development and convective heat transfer in convergent-divergent nozzles. *Transact. Am. Soc. Mech. Eng.*, 2022. **77**(8), 1235–1244. doi:10.1115/1.4014652.
- Bartz, D.R. A simple equation for rapid estimation of rocket nozzle convective heat transfer coefficients. *J. Jet Propulsion*, 1957. **27**(1), 49–53. doi:10.2514/8.12572.
- Nichols, R.H. & Nelson, C.C. Wall function boundary conditions including heat transfer and compressibility. *AIAA Journal*, 2004. **42**(6), 1107–1114. doi:10.2514/1.3539.
- White, F. & Christoph, G. A simple new analysis of compressible turbulent two-dimensional skin friction under arbitrary conditions. Technical Report No. AFFDL-TR-70- 133, Rhode Island Univ Kingston Dept of Mechanical Engineering and Applied Mechanics. February 1971.
- Dharavath, M.; Manna, P. & Chakraborty, D. Heat flux prediction in a kerosene fuelled scramjet combustor through CFD. *J. Aerospace Sci. Technol.*, 2018. **70**, 85–97.
- Kader, B. Temperature and concentration profiles in fully turbulent boundary layers. *Int. J. Heat and Mass Transfer*, 1981. **24**(9), 1541– 1544. doi:10.1016/0017-9310(81)90220-9.
- Zhalehrajabi, E.; Rahmanian, N. & Hasan, N. Effects of mesh grid and turbulence models on heat transfer coefficient in a convergent-divergent nozzle. *Asia-Pacific J. Chem. Eng.*, 2014. **9**(2), 265-271. doi:10.1002/apj.1767.
- Shih, T.H.; Liou, W.W.; Shabbir, A.; Yang, Z. & Zhu, J. A new k - ϵ eddy viscosity model for high Reynolds number turbulent flows. *Computers & Fluids*, 1995. **24**(3), 227–238. doi:10.1016/0045-7930(94)00032-T.
- Menter, F. Zonal two equation k - ω turbulence models for aerodynamic flows. *In 23rd Fluid Dynamics, Plasma dynamics, and Lasers Conference*, 1993, 2906. doi:10.2514/6.1993-2906.
- Menter, F.R. Two-equation eddy-viscosity turbulence models for engineering applications. *AIAA Journal*, 1994. **32**(8), 1598–1605. doi: 10.2514/3.12149.
- Back, L.; Gier, H. & Massier, P. Comparisons of experimental with predicted wall static-pressure distributions in conical supersonic nozzles. Technical Report JPL-TR-32-654.NASA, October 1964.
- Back, L.; Gier, H. & Massier, P. Convective heat transfer in a convergent-divergent nozzle. Technical Report JPL-TR-32-415.NASA, February 1965.
- Spalding, D.B. A single formula for the “Law of the wall”. *J. Appl. Mech.*, 1961. **28**(3), 455–458. doi:10.1115/1.3641728.
- Sutherland, W. Lii. The viscosity of gases and molecular force. *The London, Edinburgh, and Dublin Philosophical Magazine and J. Sci.*, 1893. **36**(223), 507–531. doi:10.1080/14786449308620508.
- White, F.M. & Corfield, I. Viscous fluid flow, McGraw-Hill New York, 2006. 629 p.
- Settles, G. & Dodson, L. Hypersonic shock/boundary-layer interaction database. *In 22nd Fluid Dynamics, Plasma Dynamics and Lasers Conference*, 1991, 1763. doi:10.2514/6.1991-1763.
- Settles, G.S. & Dodson, L.J. Hypersonic shock/boundary-layer interaction database: new and corrected data. Pennsylvania State Univ. Report No. 177638. NASA, April 1994.
- Greenshields, C. OpenFOAM v9 User Guide. The OpenFOAM Foundation, London, UK, 2021.
- Makhija, A.; Bodi, K. & Chakraborty, D. Heat flux prediction of hypersonic flow over a 34° compression corner using OpenFOAM®. *In 25th AIAA International Space Planes and Hypersonic Systems and Technologies Conference*, 2023, 3047. doi:10.2514/6.2023-3047.
- Makhija, A.; Bodi, K. & Sekar, T.C. Numerical simulation of heat transfer for a diamond airfoil in hypersonic flow. *In 25th AIAA International Space Planes and Hypersonic Systems and Technologies Conference*, 2023, 3048. doi:10.2514/6.2023-3048.
- Gomez, S.; Graves, B. & Poroseva, S. On the accuracy of rans simulations of 2D boundary layers with OpenFOAM. *In 44th AIAA Fluid Dynamics Conference*, 2014, 2087. doi:10.2514/6.2014-2087.

ACKNOWLEDGEMENT

We would like to acknowledge the use of the computing resources at ACE Facility, Aerospace Engineering Dept., IIT Bombay. We also acknowledge the reviewers for their invaluable input, which helped us improve the manuscript's quality.

CONTRIBUTORS

Mr Amit Makhija is a Ph.D. student in the Department of Aerospace Engineering at the IIT Bombay, Mumbai, India. His research includes: Computational fluid dynamics, combustion modelling, high-speed flow simulations, and conjugate heat transfer study in open-source software.

He contributed to the conceptualisation, numerical investigation, and writing the draft for the present study.

Dr Kowsik Bodi obtained his PhD in Aerospace Engineering from the University of California, San Diego. He is an Associate Professor of Aerospace Engineering at the IIT, Bombay, Mumbai, Maharashtra. His research interests are modelling and numerical simulations of hypersonic and high enthalpy flow and plasma applications in propulsion and flow control.

His contributions for the present work include: Conceptualizing the work and providing guidance, results, and draft review.

Prof Debasis Chakraborty obtained his PhD in Aerospace Engineering from the IIS, Bengaluru. He is presently a Professor of Mechanical and Aerospace Engineering at Mahindra University, Hyderabad, Telangana. His research interests are CFD, aerodynamics, high-speed combustion, and propulsion. His contributions for the present work include: Conceptualizing the work and providing guidance, results, and draft review.